

Boosting efficiency in light-driven water splitting by synchronizing reaction and transport processes through dynamic irradiation

Maximilian Sender,^{[a]‡} Fabian L. Huber,^{[b]‡} Maximilian C. G. Moersch,^[a, b] Simon Kaufhold,^[b] Dirk Ziegenbalg^{*[a]} and Sven Rau^{*[b]}

[a] M. Sender, M. C. G. Moersch, Prof. Dr. D. Ziegenbalg
Institute of Chemical Engineering
Ulm University
Albert-Einstein-Allee 11, 89081 Ulm, Germany
E-mail: dirk.ziegenbalg@uni-ulm.de

[b] F. L. Huber, M. C. G. Moersch, Dr. Simon Kaufhold, Prof. Dr. S. Rau
Institute of Inorganic Chemistry I
Ulm University
Albert-Einstein-Allee 11, 89081 Ulm, Germany
E-mail: sven.rau@uni-ulm.de

‡ These authors contributed equally to this work

Abstract

This work elaborates the effect of dynamic irradiation and enhanced mass transport on light-driven molecular water oxidation to counteract catalyst deactivation. It highlights the importance of overall reaction design to overcome limiting factors in artificial photosynthesis reactions. Systematic investigation of a homogenous three component ruthenium-based water oxidation system revealed significant potential to enhance the overall catalytic efficiency by synchronizing the timescales of photoreaction and mass transport in a capillary flow reactor. The overall activity could be improved by a factor of more than 10 with respect to the turnover number and a factor of 21 referring to the external energy efficiency by applying low irradiation intensities and high flow rates.

Main Text

Photocatalytic reactions have received tremendous attention from both academia and industry as sunlight presents an abundant and sustainable energy source.^[1,2] The light-driven splitting of water into oxygen and hydrogen – artificial photosynthesis – is a promising approach to supply renewable fuels and feedstock to the economy.^[3] Many heterogeneous and homogenous systems for the photochemical splitting of water have been developed and chemically optimized in regard to molecular components, buffer conditions and pH-ranges.^[4–8] Artificial photosynthetic reactions are so far usually broken down into two half reactions, which are studied separately: Oxidation of water to form oxygen, protons and electrons and reduction of protons to yield hydrogen.^[9] The overall performance of photocatalytic reactions depends on a complex interplay between molecular properties of the involved chemical species, the environment around the active components and the presence of light of suitable intensity and wavelength. The highly ordered and synchronized mechanisms of biological photosynthesis can serve as a source of inspiration: to unleash the full potential of artificial photosynthetic catalysis, a thorough understanding of the interaction between the catalytic species, the micro- and macroscopic mass transport as well as the radiation field is necessary.^[10] Thus, catalyst development and reaction engineering need to be combined synergistically.^[11–13]

To understand the impact of mass transport and irradiation conditions on the photocatalytic water oxidation, we adopted the well-known system consisting of [Ru(dpp)(pic)₂](PF₆)₂ (**Ru(dpp)**, dpp = 2,9-

di(pyridine-2'-yl)-1,10-phenanthroline, pic = 4-picoline, 2.6 μM), which acts as single-site water oxidation catalyst (WOC), the photosensitizer $[\text{Ru}(\text{dceb})_2(\text{bpy})](\text{PF}_6)_2$ (**PS**, dceb = diethyl[2,2'-bipyridine]-4,4'-dicarboxylate, bpy = 2,2'-bipyridine, 0.3 mM) and $\text{Na}_2\text{S}_2\text{O}_8$ (10 mM) as sacrificial electron-acceptor in a solvent mixture of 96 v-% of aqueous H_3BO_3 / NaHCO_3 buffer (pH 6.5, 0.08 M H_3BO_3) and 4 v-% MeCN (Fig. 1 a).^[14–16]

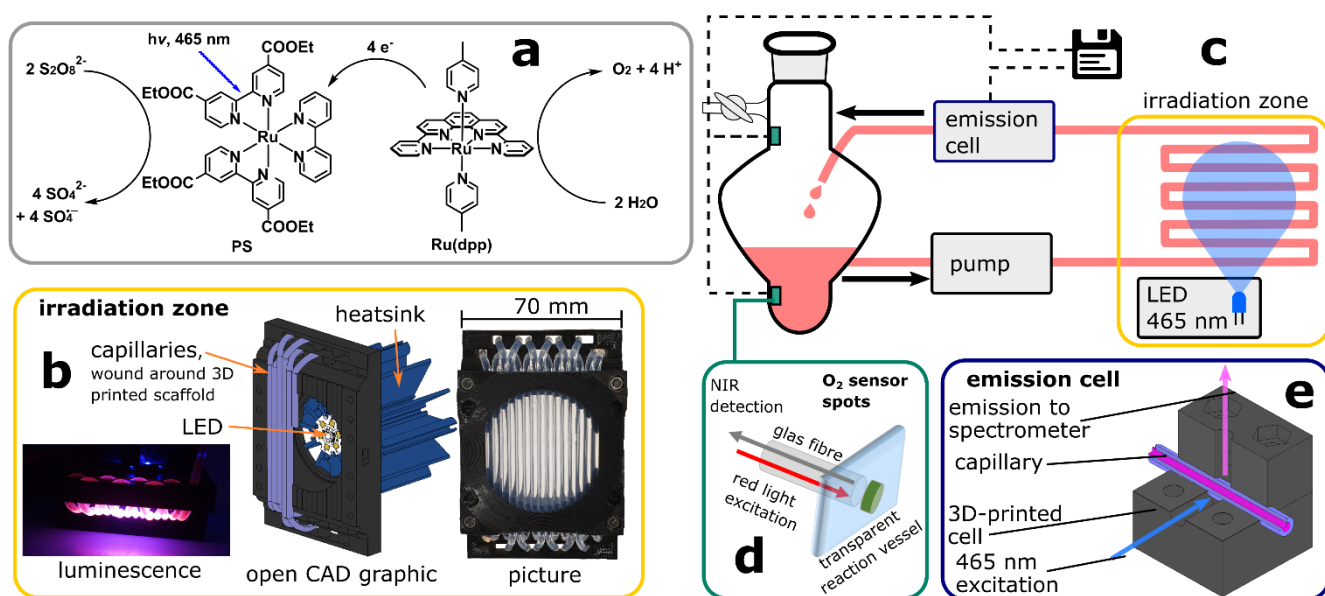


Figure 1. Illustration of the homogenous three component water oxidation system (a) and schematic depiction of the capillary flow-through-reactor setup (b – e).

A novel capillary flow-through reactor design, operated in recycling mode, is used to study the impact of flow rate and light intensity on the performance of a molecular system for light-driven water oxidation (Fig. 1).^[17–21] In this reactor system the reaction mixture is cycled from the storage vessel through a capillary which is wound in a 3D-printed scaffold.^[22,23] The parallel arrangement of the capillary creates a defined projection area that is adapted to the emission characteristics of the light source (Fig. 1 c and b). Oxygen formation was monitored in solution as well as in the gas phase by an optical sensor (Fig. 1 d).^[17] Integrity of the PS was monitored by tracing its emission *in situ* with a clamp-on emission cell (Fig. 1 e). Further details on the setup are given in the ESI.

The influence of the operating conditions on the catalytic performance was studied systematically by varying the flow rates of the reaction mixture and irradiation intensity of the light source. While passing through the capillary, the reaction solution passes through irradiated and non-irradiated parts of the reactor (compare Figure 1 b). Varying the flow rate from 6 to 50 mL min^{-1} leads to average irradiation periods of 0.77 to 0.09 s and dark periods of 1.47 to 0.18 s (see Table 1; full details in ESI Table S1). Higher flow rates lead to shorter irradiation/dark periods and could thus be helpful to synchronize different reaction steps. Additionally, the light intensity could be adjusted through variation of the radiant power of the LED. Both parameters directly influence the reaction rate and with this the interaction of mass transport and reaction rate as well.

The catalytic performance of the system was determined by four parameters: turnover number (TON, amount of product per catalyst), turnover frequency (TOF, TON per time interval), as well as external energetic (ξ_E) and photonic efficiencies (ξ_p), referring to the amount of product in regard to energy consumed or photons emitted by the light source (detailed description in ESI).

Table 1. Mean pulse durations in the scaffold for different flow rates.

flow rates /(mL/min)	mean irradiation pulses /s	Mean irradiation pauses /s
6	0.77	1.47
17	0.27	0.52
21	0.22	0.42
29	0.16	0.30
50	0.090	0.18

For other catalytic systems, an increase of irradiation intensity also leads to an increase in catalytic performance,^[24] however, in our case, lower irradiation intensity generally lead to higher maximum TONs. This effect is most pronounced when high flow rates are applied (c.f. Fig. 2a). By changing the operating conditions, the TONs could be increased by a factor of more than 11 from 33 (6 mL min⁻¹, 0.76 W) to 378 (50 mL min⁻¹, 0.22 W). These changes in performance become more obvious when analyzing the efficiency parameters ξ_E and ξ_p . A 21-fold increase in external energetic efficiency form around 2 $\mu\text{mol Wh}^{-1}$ to 42 $\mu\text{mol Wh}^{-1}$ was found. ξ_p increases from 0.7 % to 17 %, representing a 24-fold increase of the external photonic efficiency. The even more pronounced increase is attributed to the higher efficiency of the LED at lower current.

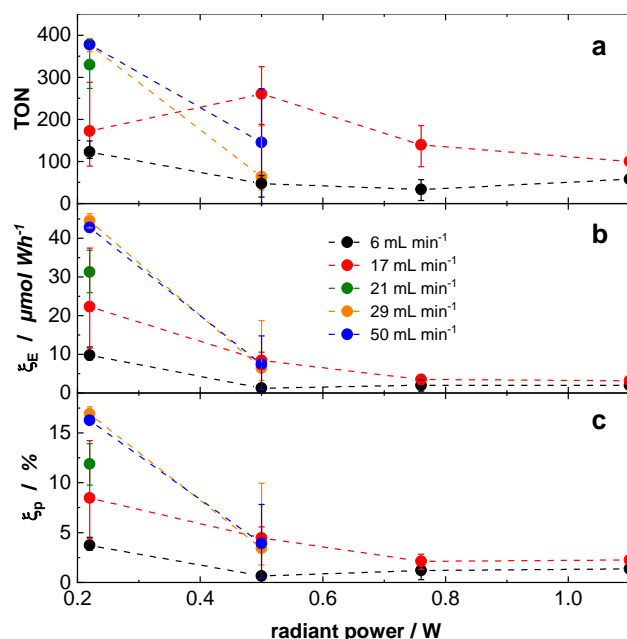


Figure 2. Impact of different flow rates and light intensities on the photocatalytic performance. Dotted lines added for visual clarity. **a:** Results given in maximum TON achieved, each point was measured at least three times. **b:** Results in external energetic efficiency (ξ_E). **c:** Results in external photonic efficiency (ξ_p).

It is very clear from these analyses, that excess photons are detrimental for the overall performance. A possible explanation is that excess light could drive competing side reactions, which destabilize the catalytic system and lead to its premature deactivation.^[25] A likely deactivation pathway for ruthenium polypyridine **PSs** is ligand photosubstitution.^[26–28]

The **PS** shows visible emission with a maximum at 635 nm (Fig. S7), while **Ru(dpp)** is not emissive.^[14] As an indicator for functionality of the **PS**, emission of the reaction solution was measured with a clamp-on emission cell (see ESI) *in situ*. A comparison of TOF and emission intensity is shown in Figure 3. Within 90 minutes, the emission drops to about 10% of its original intensity and clearly correlates with the decreasing TOF.

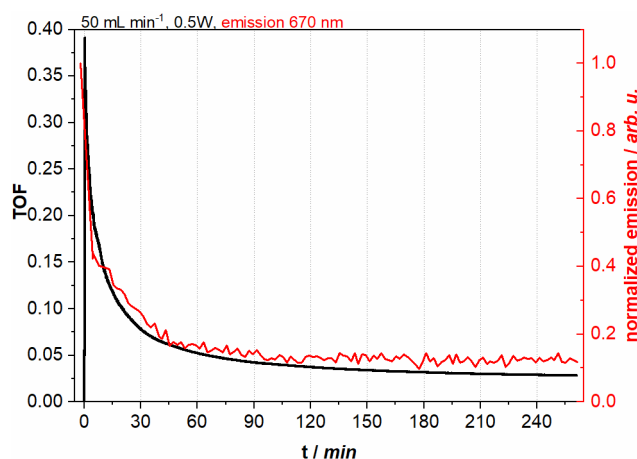


Figure 3. Luminescence at 670 nm (red, see Fig. S7 for emission spectrum of the **PS**) and TOF over time (black). Measurements were performed at 50 mL min⁻¹ and 0.5 W.

These observations indicate destruction of the **PS** to such a low level that catalytic turnover is no longer promoted efficiently. Comparative measurements conducted at different light intensities show a fast breakdown of the catalytic activity for high irradiation intensity (Fig. 4). At a flow rate of 6 mL min⁻¹ and a radiant power of 1.1 W the maximum TON of 60 was reached in around 10 min, while at 0.22 W radiation power the maximum TON of approximately 110 was reached after 65 min (Fig. 4 **a**). Accordingly, TOF at 1.1 W intensity reached 0.38 s⁻¹ and declined fast after reaching maximum activity. While at 0.22 W a maximum TOF of only 0.09 s⁻¹ was reached but maintained over a prolonged period (Fig. 4 **b**). Measurements at different flow-rates generally showed the same trend.

To understand the factors determining the activity and long-term stability, further investigations were pursued. For higher flow rates not only shorter irradiation and dark phases have to be considered, but also a more efficient mass transport, which in turn improves catalytic performance by overcoming diffusion limitations. Beside this, secondary flows are induced at higher flow rates in the windings that break up the typical laminar flow conditions and induce radial mass transport in the capillaries as well.^[29] This additionally reduces the impact of steep intensity gradients in the irradiation zone. Thus, for flow rates of 29 mL min⁻¹ and above, mass transport reaches an ideal level for the investigated irradiation intensity range.

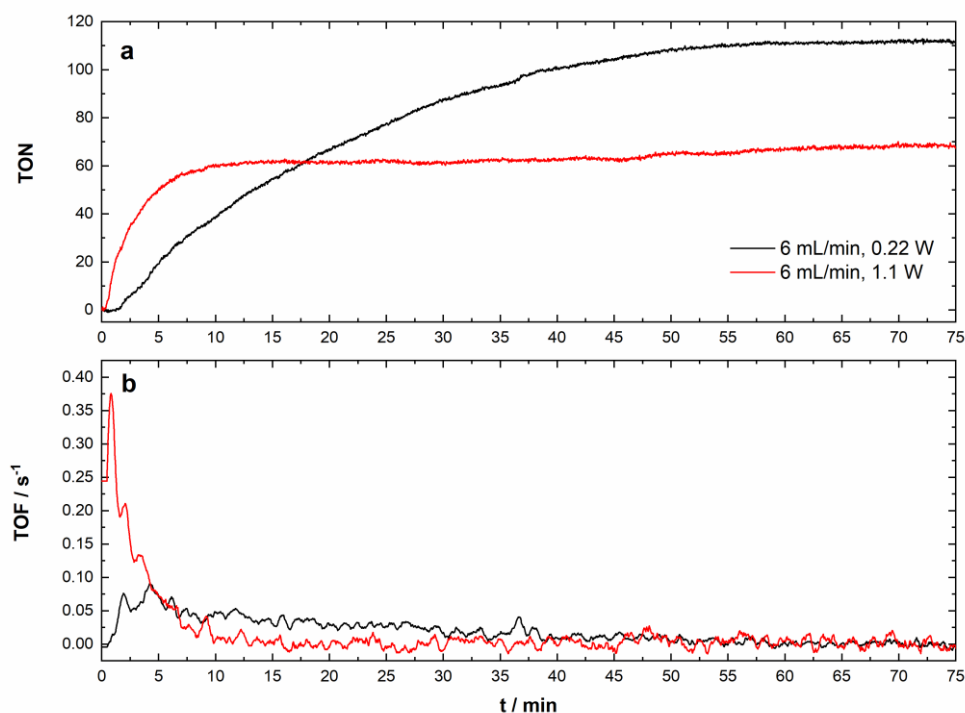


Figure 4. Comparison of TON (a) and TOF (b) between measurements at 0.22 W (black) and 1.1 W radiation power, conducted at a flow rate of 6 mL min⁻¹.

To further investigate the influence of mass transport, a reference experiment was conducted by irradiating the catalytic solution in a closed vial under stirred and not-stirred conditions.^[17] A custom made stirrer was used to ensure intense stirring of the entire solution. Although the vial-setup is only of limited comparability to the more complex capillary reactor, the TON is roughly doubled from around 110 to 230 when stirring the solution (see ESI). While these experiments do not address the possible influence of light and dark periods, it still indicates the positive influence of increased mass transport.

In our study we show that photon flux management is a powerful tool to bring photocatalytic water splitting reaction performance to a new level. By reducing the irradiation intensity and improving mass transport through high flow rates in our capillary photoreactor, an improved synchronization of different reaction steps is achieved. This improvement is reflected in a 11-fold increase in TON and is even more pronounced for the external photonic efficiency, here a 20-fold increase is achieved. Thus, we show for the first time the synergistic effect of molecular and macroscopic reaction engineering in light driven water splitting reactions with molecular catalysts. With ever more elaborated (photo)catalysts being developed, it is clear that tuning reaction conditions on all relevant scales will play a crucial part in achieving maximum performance of the catalytic system, especially in view of the future industrial application of such processes. While the complex apparatus of biological photosynthesis features mechanisms to synchronize different reactions steps and protect or repair light-harvesting units, this is often not the case in artificial photosynthesis.^[30–33] Here the oxidative half reaction usually proceeds on a much shorter timescale than the reductive half reaction.^[34] Smart reaction design and engineering will help to overcome these limitations.

Acknowledgements

This research was funded by the Deutsche Forschungsgemeinschaft DFG as part of the collaborative research center TRR234 "CataLight" (364549901), project A1, A4 and C6.

Keywords: photocatalysis • photoreaction engineering • water oxidation • flow-chemistry • ruthenium

References

- [1] M. Oelgemöller, *Chem. Rev.* **2016**, *116*, 9664–9682.
- [2] D. Cambie, C. Bottecchia, N. J. W. Straathof, V. Hessel, T. Noe, *Chem. Rev.* **2016**, *116*, 10276–10341.
- [3] N. S. Lewis, D. G. Nocera, *Proc. Natl. Acad. Sci. U. S. A.* **2006**, *103*, 15729–15735.
- [4] A. Kudo, Y. Miseki, *Chem. Soc. Rev.* **2009**, *38*, 253–278.
- [5] R. Matheu, P. Garrido-Barros, M. Gil-Sepulcre, M. Z. Ertem, X. Sala, C. Gimbert-Suriñach, A. Llobet, *Nat. Rev. Chem.* **2019**, *3*, 331–341.
- [6] J. Ran, J. Zhang, J. Yu, M. Jaroniec, S. Z. Qiao, *Chem. Soc. Rev.* **2014**, *43*, 7787–7812.
- [7] W. T. Eckenhoff, R. Eisenberg, *Dalt. Trans.* **2012**, *41*, 13004–13021.
- [8] M. D. Kärkäs, O. Verho, E. V. Johnston, B. Åkermark, *Chem. Rev.* **2014**, *114*, 11863–12001.
- [9] M. Schulz, M. Karnahl, M. Schwalbe, J. G. Vos, *Coord. Chem. Rev.* **2012**, *256*, 1682–1705.
- [10] A. N. Tikhonov, *Cell Biochem. Biophys.* **2017**, *75*, 421–432.
- [11] F. Guba, T. Ümit, K. Gugeler, M. Buntrock, T. Rommel, D. Ziegenbalg, *Chemie Ing. Tech.* **2019**, *91*, 17–29.
- [12] I. Reim, B. Wriedt, Ü. Tastan, D. Ziegenbalg, M. Karnahl, *ChemistrySelect* **2018**, *3*, 2905–2911.
- [13] S. Meyer, D. Tietze, S. Rau, B. Schäfer, G. Kreisel, *J. Photochem. Photobiol. A Chem.* **2007**, *186*, 248–253.
- [14] R. Zong, R. P. Thummel, *J. Am. Chem. Soc.* **2004**, *126*, 10800–10801.
- [15] L. Tong, R. Zong, R. Zhou, N. Kaveevivitchai, G. Zhang, R. P. Thummel, *Faraday Discuss.* **2015**, *185*, 87–104.
- [16] J. T. Muckerman, M. Kowalczyk, Y. M. Badiei, D. E. Polyansky, J. J. Concepcion, R. Zong, R. P. Thummel, E. Fujita, *Inorg. Chem.* **2014**, *53*, 6904–6913.
- [17] F. L. Huber, S. Amthor, B. Schwarz, B. Mizaikoff, C. Streb, S. Rau, *Sustain. Energy Fuels* **2018**, *2*, 1974–1978.
- [18] J. P. Knowles, L. D. Elliott, K. I. Booker-Milburn, *Beilstein J. Org. Chem.* **2012**, *8*, 2025–2052.
- [19] C. Sambiagio, T. Noël, *Trends Chem.* **2020**, *2*, 92–106.
- [20] K. Loubière, M. Oelgemöller, T. Aillet, O. Dechy-Cabaret, L. Prat, *Chem. Eng. Process. - Process Intensif.* **2016**, *104*, 120–132.
- [21] L. D. Elliott, J. P. Knowles, P. J. Koovits, K. G. Maskill, M. J. Ralph, G. Lejeune, L. J. Edwards, R. I. Robinson, I. R. Clemens, B. Cox, D. Pascoe, G. Koch, M. Eberle, M. B. Berry, K. I. Booker-Milburn, *Chemistry* **2014**, *20*, 15226–15232.
- [22] M. Sender, D. Ziegenbalg, *React. Chem. Eng.* **2021**, DOI 10.1039/D0RE00457J.
- [23] M. Sender, B. Wriedt, D. Ziegenbalg, *React. Chem. Eng.* **2021**, DOI 10.1039/D0RE00456A.
- [24] M. G. Pfeffer, T. Kowacs, M. Wächter, J. Guthmüller, B. Dietzek, J. G. Vos, S. Rau, *Angew. Chemie - Int. Ed.* **2015**, *54*, 6627–6631.
- [25] H. E. Bonfield, T. Knauber, F. Lévesque, E. G. Moschetta, F. Susanne, L. J. Edwards, *Nat. Commun.* **2020**, *11*, 1613.
- [26] A. Soupart, F. Alary, J.-L. Heully, P. I. P. Elliott, I. M. Dixon, *Inorg. Chem.* **2020**, DOI 10.1021/acs.inorgchem.0c01843.
- [27] A. Vaidyalingham, P. K. Dutta, *Anal. Chem.* **2000**, *72*, 5219–5224.
- [28] A. Juris, V. Balzani, F. Barigelli, S. Campagna, P. Belser, A. von Zelewsky, *Coord. Chem. Rev.* **1988**, *84*, 85–277.
- [29] P. Hermann, J. Timmermann, M. Hoffmann, M. Schlüter, C. Hofmann, P. Löb, D. Ziegenbalg, *Chem. Eng. J.* **2018**, *334*, 1996–2003.
- [30] L. T. Hickey, A. N. Hafeez, H. Robinson, S. A. Jackson, S. C. M. Leal-Bertioli, M. Tester, C. Gao, I. D. Godwin, B. J. Hayes, B. B. H. Wulff, *Nat. Biotechnol.* **2019**, *37*, 744–754.
- [31] N. C. Rockwell, Y. S. Su, J. C. Lagarias, *Annu. Rev. Plant Biol.* **2006**, *57*, 837–858.
- [32] A. I. Velez-Ramirez, W. Van Ieperen, D. Vreugdenhil, P. M. J. A. Van Poppel, E. Heuvelink, F. F. Millenaar, *Nat. Commun.* **2014**, *5*, DOI 10.1038/ncomms5549.
- [33] A. I. Velez-Ramirez, W. Van Ieperen, D. Vreugdenhil, F. F. Millenaar, *Trends Plant Sci.* **2011**, *16*, 310–318.
- [34] R. Matheu, M. Z. Ertem, C. Gimbert-Suriñach, X. Sala, A. Llobet, *Chem. Rev.* **2019**, *119*, 3453–3471.